Glaucoma Detection Ability of Macular Ganglion Cell-Inner Plexiform Layer Thickness in Myopic Preperimetric Glaucoma

Bo Ram Seol, Jin Wook Jeoung, and Ki Ho Park

Department of Ophthalmology, Seoul National University Hospital, Seoul National University College of Medicine, Seoul, Korea

Correspondence: Ki Ho Park, Department of Ophthalmology, Seoul National University Hospital, Seoul National University College of Medicine, 101 Daehak-ro, Chongno-gu, Seoul 110-744, Republic of Korea; kihopark@snu.ac.kr.

Submitted: September 8, 2015
Accepted: November 19, 2015

Citation: Seol BR, Jeoung JW, Park KH. Glaucoma detection ability of macular ganglion cell-inner plexiform layer thickness in myopic preperimetric glaucoma. *Invest Ophthalmol Vis Sci*. 2015;56:8306–8313. DOI:10.1167/iovs.15-18141

Purpose. We evaluated the glaucoma detection ability of macular ganglion cell–inner plexiform layer (GCIPL) thickness measured by spectral-domain optical coherence tomography (SD-OCT) and compared it to peripapillary retinal nerve fiber layer (RNFL) thickness and optic nerve head (ONH) parameters in myopic preperimetric glaucoma (PPG).

Methods. We analyzed 353 eyes, including 67 nonmyopic preperimetric glaucomatous eyes, 182 myopic healthy eyes, and 104 myopic preperimetric glaucomatous eyes. Myopic PPG detection abilities of the respective parameters were assessed by calculating the area under receiver operating characteristic (AUROC) curves. The myopic eyes were divided into two groups (a nonhighly myopic and a highly myopic group). The diagnostic performance was analyzed for each group independently, and differences between the two groups also were evaluated.

Results. The best parameter for discrimination of myopic PPG from myopic healthy eyes was inferotemporal macular GCIPL thickness. The AUROCs of this parameter were 0.752, 0.747, and 0.737 in the total myopic, nonhighly myopic, and highly myopic groups, respectively. These were significantly larger than the AUROCs of the other parameters, including average RNFL thickness, average GCIPL thickness, rim area, inferior RNFL thickness, and minimum GCIPL thickness (P = 0.021, 0.012, 0.016, 0.036, and 0.013, respectively). The inferotemporal macular GCIPL thickness showed no significant difference between nonhighly myopic and highly myopic groups.

Conclusions. The inferotemporal macular GCIPL thickness was the best PPG-detection parameter for myopic eyes. Inferotemporal macular GCIPL thickness evaluation can be considered to be a useful means of diagnosing PPG in myopic eyes.

Keywords: glaucoma detection ability, optical coherence tomography, myopic preperimetric glaucoma

In myopic eyes, evaluation of glaucomatous structural change is difficult due to the considerable morphologic variations in the optic nerve head (ONH).[1–4] Peripapillary retinal nerve fiber layer (RNFL) thickness is known to be a useful parameter for detection of glaucoma; however, in myopic eyes, RNFL thickness measurement is inaccurate, because RNFL thickness in myopic eyes is thinner than in nonmyopic eyes.[5–10] Thus, a more accurate morphological parameter for detection of glaucoma in myopic eyes is needed. Macular inner retinal thickness as a glaucoma detection parameter for myopic eyes has been reported to be comparable or superior to peripapillary RNFL thickness, though little is known about macular ganglion cell-inner plexiform layer (GCIPL) thickness or its diagnostic power, especially for preperimetric glaucoma (PPG) in myopic eyes.[11–16]

Diagnosing PPG is problematic, as it is in the earliest stage of glaucoma. Diagnosis of glaucoma in myopic eyes is known to be difficult due to myopic eye's characteristic disc tilting, large ovality index, shallow and large cup, and large peripapillary crescent.[4,17] Obviously then, a more effective PPG-detection parameter for myopic eyes would be very helpful to clinicians.

Recently, Choi et al.[18] reported that in cases of high myopia, the glaucoma detection ability of macular GCIPL thickness was high and comparable to that of peripapillary RNFL thickness. The overall median MD rate was −7.44 dB in their glaucoma group. As far as we know, there has been as yet no report on the diagnostic ability of macular GCIPL with respect to myopic PPG. Therefore, we investigated the diagnostic ability of a number of macular GCIPL thickness parameters to differentiate PPG from healthy eyes, and compared the results to those for other RNFL thickness and ONH parameters.

Methods

Subjects

This retrospective cross-sectional study included 353 eyes: 67 nonmyopic preperimetric glaucomatous eyes (NGE), 182 myopic healthy eyes (MHE), and 104 myopic preperimetric glaucomatous eyes (MGE). All of the participants were examined at the Glaucoma Clinic of Seoul National University Hospital between October 2011 and March 2015. The study protocol, approved by the Institutional Review Board of Seoul

National University Hospital, adhered to the tenets of the Declaration of Helsinki.

All of the subjects underwent a complete ophthalmic examination, which included visual acuity (VA) and IOP measurement (by Goldmann applanation tonometry), corneal pachymetry (Pocket II Pachymeter Echo Graph; Quantel Medical, Clermont-Ferrand, France), noncycloplegic refraction (Autorefractor KR-8900; Topcon Corporation, Tokyo, Japan), measurement of axial length (AXL; Axis II PR; Quantel Medical, Inc., Bozeman, MT, USA), slit-lamp examination, gonioscopy, dilated fundus examination, color disc photography, red-free RNFL photography (Vx-10; Kowa Optimed, Tokyo, Japan), Humphrey Visual Field Analyzer (Carl Zeiss Meditec, Inc., Dublin, CA, USA) using the Swedish interactive threshold algorithm with the 30-2 standard program, and a spectral-domain optical coherence tomography (SD-OCT) device (Carl Zeiss Meditec, Inc.). In the myopic eyes, the refraction data were converted to spherical equivalents (SE), on which basis the subjects were divided into two groups: a nonhighly myopic group (SE $>$–6.00 diopters [D] and $\leq$–0.50 D) and a highly myopic group (SE $\leq$–6.00 D).

The inclusion criteria for glaucoma patients were age greater than 18 years, best-corrected visual acuity (BCVA) of at least 20/40 in the examined eyes and gonioscopy-confirmed open angle. Patients were excluded for any of the following reasons: history of ocular surgery or any other systemic or ocular disease. For subjects in whom both eyes met the inclusion criteria, one was selected randomly for further examination. Preperimetric glaucomatous eyes were defined as eyes with one or more localized RNFL defect corresponding to glaucomatous optic disc changes and a normal VF test. Glaucomatous optic disc changes were defined on stereoscopic color disc photography as cup/disc (C/D) asymmetry between the glaucomatous and normal eyes of greater than 0.2, large cupping ($>$0.7 vertical C/D ratio), neuroretinal rim thinning, notching, or excavation. The stereoscopic disc photography was assessed by two glaucoma specialists (SBR, PKH) in a masked fashion, without knowledge of the clinical data or SD-OCT results. Only subjects classified by both observers as manifesting glaucomatous optic disc changes were included in the study. A reliable VF, defined as fixation losses less than 20%, and each of the false-positive and false-negative rates less than 15%, was used. A normal VF was defined as a mean deviation (MD) and pattern standard deviation (PSD) within the 95% confidence limit and a glaucoma hemifield test result within the normal limits. Only those subjects who did not show repeatable VF loss were finally included.

Healthy eyes were defined as those with no history of ocular disease or ocular surgery. Healthy eyes also showed an IOP less than 22 mm Hg, an absence of glaucomatous optic disc change, or RNFL defect as determined by two glaucoma specialists (SBR, PKH), and no perimetric defects.

SD-OCT Measurements

Spectral domain-OCT images of macular scans (macular cube 200 $\times$ 200 protocol) and of peripapillary RNFL scans (optic disc cube 200 $\times$ 200 protocol) were obtained by a Cirrus SD-OCT (Carl Zeiss Meditec, Inc.) device with version 6.0 software. Images with a signal strength of 6 or greater and well-centered on the optic disc or fovea were included.

The ganglion cell analysis (GCA) algorithm included in the SD-OCT device software was used to measure macular GCIPL thickness within a 6 $\times$ 6 $\times$ 2 mm cube centered on the fovea. The sectoral thicknesses of the GCIPL are measured in an elliptical annulus (diameter; an inner vertical diameter of 1 mm, outer diameter of 4 mm, and an inner horizontal diameter of 1.2 mm and outer diameter of 4.8 mm).[19–21]

The optic disc cube image is acquired through a 6 $\times$ 6 $\times$ 2 mm cube of data consisting of 200 $\times$ 200 axial scans. From these data, the system extracts a B-scan in the shape of a circle of 3.46 mm diameter, and the algorithm automatically detects the center of the optic disc and placed it around the optic disc.[22] The system calculates the RNFL thickness at each point on the circle and displays the measured values.[22]

The macular GCIPL thickness measurements were analyzed according to the average, minimum, and sectoral (superonasal, superior, superotemporal, inferotemporal, inferior, inferonasal) parameters. As for the peripapillary RNFL thickness measurements, the average, superior, inferior, temporal, and nasal quadrant thicknesses along with the 12 clock-hour thickness were included in the analysis. In the ONH measurements, the individual parameters were rim area, disc area, average C/D ratio, vertical C/D ratio, and cup volume.

Statistical Analysis

All of the peripapillary RNFL thickness, macular GCIPL thickness, and ONH parameters were compared between the NGE and MGE and between the MHE and MGE using the Student's *t*-test for independent variables. Additionally, the two myopic groups (nonhighly and highly myopic) were compared for each of the individual parameters.

To investigate the diagnostic ability of all of the parameters, area under the receiver operating characteristic (AUROC) curves were calculated. These AUROCs were compared between the two groups (nonhighly and highly myopic) using the methods described by DeLong et al.[23] Then, the AUROC differences of the best parameter and of all of the other parameters were tested using a statistical software package (MedCalc v. 12.0; MedCalc Statistical Software, Marakierke, Belgium). All of the other statistical analyses were performed using statistical analysis software (SPSS 18.0; SPSS, Inc., Chicago, IL, USA); *P* values less than 0.05 were considered statistically significant.

Results

Subjects

A total of 353 eyes (67 NGE, 182 MHE, and 104 MGE) were included in this study. The demographics and baseline characteristics are summarized in Table 1. In the comparison of the NGE and MGE, there were no statistically significant differences in age, baseline IOP, central corneal thickness (CCT), MD, or PSD. Spherical equivalent and AXL showed statistically significant differences ($P < 0.001$ and $P < 0.001$, respectively). In the comparison of the MHE and MGE, there were no statistically significant differences in age, baseline IOP, CCT, SE, or AXL. Mean deviation and PSD showed no statistically significant differences.

SD-OCT Measurements

The results of comparisons of the macular GCIPL thickness, peripapillary RNFL thickness, and ONH parameters between the NGE and MGE and between the MHE and MGE are shown in Table 2 and Supplementary Table S1.

Macular GCIPL Thickness

The MGEs were thinner than the NGEs in all regions of the macular GCIPL. The average macular GCIPL thickness and inferonasal, inferior, and inferotemporal regions showed

Table 1. Demographic Characteristics of Study Subjects

	Total Eyes $n = 353$	NGE: Group 1 $n = 67$	MHE: Group 2 $n = 182$	MGE: Group 3 $n = 104$	*P* Value: NGE vs. MGE: Group 1 vs. 3	*P* Value: MHE vs. MGE: Group 2 vs. 3
Mean age ± SD, y	49.24 ± 10.82	51.90 ± 7.79	47.65 ± 12.06	50.30 ± 9.76	0.261	0.057
Sex, men/women	192/161	29/38	101/81	62/42		
In baseline phase						
IOP ± SD, mm Hg	15.21 ± 3.22	15.27 ± 1.94	15.05 ± 3.27	15.48 ± 3.79	0.672	0.333
CCT ± SD, μm	545.60 ± 31.18	540.48 ± 31.19	551.58 ± 33.59	542.89 ± 27.88	0.618	0.053
MD ± SD	−0.11 ± 1.45	0.09 ± 1.63	−0.07 ± 1.26	−0.31 ± 1.63	0.110	0.182
PSD ± SD	1.90 ± 0.61	1.93 ± 0.46	1.92 ± 0.92	1.92 ± 0.65	0.965	0.511
SE ± SD, diopter	−2.92 ± 3.07	0.66 ± 1.04	−3.72 ± 2.77	−3.84 ± 2.77	< 0.001*	0.709
AXL ± SD, mm	24.52 ± 1.45	23.42 ± 0.88	25.00 ± 0.88	25.32 ± 1.30	< 0.001*	0.242

SD, standard deviation.
* Value for comparison of nonmyopic and myopic preperimetric glaucomatous eyes using Student's *t*-test.

statistically significant differences ($P = 0.016$, 0.008, 0.005, and 0.028, respectively). The MGEs were thinner than the MHEs in all regions of the macular GCIPL (all $P < 0.05$).

In the nonhighly myopic group, macular GCIPL thickness showed statistically significant differences between the MGE and MHE (all $P < 0.05$). In the highly myopic group, the macular GCIPL thickness parameters showed statistically significant differences between the MGE and MHE, except for superior GCIPL ($P = 0.091$) and inferonasal GCIPL ($P = 0.359$) thickness. In the intergroup comparison, the nonhighly and highly myopic groups showed significant differences in all parameters (all $P < 0.05$).

Peripapillary RNFL Thickness

In the main RNFL thickness parameters, the MGEs were thinner than the NGEs in all regions of the RNFL except the temporal region. Only the temporal RNFL thickness of the MGE was thicker than that of the NGE ($P = 0.006$). The MGEs were significantly thinner than MHEs in all regions of the RNFL (all $P < 0.05$). In the clock-hour RNFL thickness parameters, the MGE was thinner than the NGE in the 12, 7, 6, 5, 4, 3, 2, and 1 o'clock sectors of the RNFL. Statistically significant differences were found in the 6, 4, 2, and 1 o'clock sectors of the RNFL ($P = 0.002$, 0.005, 0.003, and 0.013, respectively). In the comparison of the MGE and MHE, the MGE was thinner than the MHE in all regions of the RNFL. Statistically significant differences were found in the 10, 7, 6, 5, 4, 2, and 1 o'clock RNFL thickness sectors ($P = 0.003$, < 0.001, < 0.001, 0.003, 0.003, 0.002, and 0.003, respectively).

In the nonhighly myopic group, statistically significant differences were found for all of the peripapillary RNFL clock-hour thicknesses excepting 12, 11, 9, and 3 o'clock ($P = 0.192$, 0.096, 0.271, and 0.507, respectively). There were no statistically significant differences in main RNFL thickness. In the highly myopic group, significant differences were found only in average, nasal, inferior, and 6 o'clock RNFL thicknesses ($P = 0.045$, 0.046, 0.048, and 0.032, respectively). Comparison of the nonhighly and highly myopic groups showed significant differences in average, superior, inferior, and 12, 6, 5, 2, and 1 o'clock RNFL thicknesses ($P = 0.004$, 0.011, 0.002, 0.048, < 0.001, 0.023, 0.017, and 0.023, respectively).

ONH Parameters

Comparing the NGE and MGE groups, all of the ONH parameters except rim area ($P = 0.142$) showed statistically significant differences. When comparing the MHE and MGE groups, rim area ($P < 0.001$), and average ($P = 0.008$) and vertical ($P = 0.012$) C/D ratios showed statistically significant differences, whereas disc area and cup volume did not.

In the nonhighly myopic group, rim area ($P < 0.001$), and average ($P = 0.009$) and vertical ($P = 0.049$) C/D ratios showed statistically significant differences, while in the highly myopic group, only rim area ($P = 0.017$) showed statistically significant differences. Comparison of the nonhighly and highly myopic groups showed statistically significant differences in disc area ($P = 0.001$) and cup volume ($P = 0.003$).

Diagnostic Ability

The AUROC curves of the SD-OCT parameters are listed in Table 3, Supplementary Table S2. The GCIPL parameters showed better diagnostic ability than did the RNFL and ONH parameters. Inferotemporal GCIPL thickness was the best parameter for detection of PPG in myopic eyes.

Macular GCIPL Thicknesses

In the nonhighly and highly myopic groups, all of the GCIPL thicknesses showed an AUROCs above 0.5. The inferotemporal GCIPL parameter showed the highest AUROCs. In the total, nonhighly, and highly myopic groups, the AUROC values were 0.752, 0.747, and 0.737, respectively. Between the nonhighly and highly myopic groups, there were no significant AUROC value differences.

Peripapillary RNFL Thicknesses

In the highly myopic group, all of the peripapillary RNFL thicknesses except temporal RNFL and 11, 9, and 8 o'clock ($P = 0.496$, 0.469, 0.497, and 0.420, respectively) parameters showed AUROC curves above 0.5. In the nonhighly and highly myopic groups, the inferior RNFL parameter showed the highest AUROC. The AUROCs were 0.686, 0.687, and 0.643 in the total, nonhighly, and highly myopic groups, respectively. There were no significant differences in the AUROC values between the nonhighly and highly myopic groups for any of the RNFL parameters.

ONH Parameters

Among the ONH parameters, only rim area and disc area showed AUROCs above 0.5. In the nonhighly and highly myopic groups, rim area showed the highest AUROCs. The rim

Table 2. Macular GCIPL Thickness Parameters, RNFL Thickness Parameters, and ONH Parameters Obtained by SD-OCT

					NGE vs. MGE: Group 1 vs. 3		MHE vs. MGE: Group 2 vs. 3	
	Total Eyes $n = 353$	**NGE: Group 1 $n = 67$**	**MHE: Group 2 $n = 182$**	**MGE: Group 3 $n = 104$**	**Comparison of Parameter**	***P* Value**	**Comparison of Parameter**	***P* Value**
Macular GCIPL thickness parameters, μm								
Average	78.08 ± 6.82	77.87 ± 7.26	79.78 ± 6.30	75.26 ± 6.51	Group 1 > 3	0.016*	Group 2 > 3	< 0.001†
Minimum	73.66 ± 10.23	72.42 ± 11.03	76.36 ± 8.53	69.75 ± 11.07	Group 1 > 3	0.125	Group 2 > 3	< 0.001†
Superotemporal	77.77 ± 6.56	76.91 ± 8.03	79.25 ± 5.47	75.74 ± 6.67	Group 1 > 3	0.303	Group 2 > 3	< 0.001†
Superior	78.77 ± 7.86	78.91 ± 8.10	80.04 ± 7.39	76.45 ± 8.04	Group 1 > 3	0.053	Group 2 > 3	< 0.001†
Superonasal	80.72 ± 8.10	80.64 ± 8.22	81.98 ± 7.93	78.55 ± 7.94	Group 1 > 3	0.099	Group 2 > 3	< 0.001†
Inferonasal	78.47 ± 8.01	79.42 ± 7.89	79.55 ± 7.58	75.96 ± 8.34	Group 1 > 3	0.008*	Group 2 > 3	< 0.001†
Inferior	75.59 ± 8.65	75.64 ± 8.96	77.67 ± 8.16	71.91 ± 8.12	Group 1 > 3	0.005*	Group 2 > 3	< 0.001†
Inferotemporal	77.24 ± 7.96	75.84 ± 8.31	80.17 ± 6.55	73.04 ± 7.92	Group 1 > 3	0.028*	Group 2 > 3	< 0.001†
Main RNFL thickness parameters, μm								
Average	87.68 ± 9.88	86.61 ± 11.01	90.01 ± 9.62	84.29 ± 8.46	Group 1 > 3	0.144	Group 2 > 3	< 0.001†
Superior	110.38 ± 18.02	110.45 ± 21.64	112.35 ± 17.54	106.89 ± 15.80	Group 1 > 3	0.247	Group 2 > 3	0.009†
Nasal	63.17 ± 9.14	64.12 ± 8.32	64.44 ± 9.99	60.33 ± 7.37	Group 1 > 3	0.002*	Group 2 > 3	< 0.001†
Inferior	108.57 ± 17.90	109.22 ± 19.87	112.20 ± 17.16	101.81 ± 15.97	Group 1 > 3	0.008*	Group 2 > 3	< 0.001†
Temporal	69.05 ± 13.45	62.78 ± 11.56	72.04 ± 14.17	67.56 ± 11.70	Group 3 > 1	0.006*	Group 2 > 3	0.011†
RNFL clock-hour thickness parameters, μm								
12 Superior	109.25 ± 27.36	113.82 ± 30.73	109.92 ± 26.85	105.13 ± 25.60	Group 1 > 3	0.056	Group 2 > 3	0.140
11	122.04 ± 23.84	114.19 ± 26.17	125.34 ± 22.76	121.33 ± 23.08	Group 3 > 1	0.063	Group 2 > 3	0.155
10	79.62 ± 17.82	72.04 ± 15.97	83.76 ± 18.83	77.27 ± 15.01	Group 3 > 1	0.032*	Group 2 > 3	0.003†
9 Temporal	55.85 ± 10.99	50.79 ± 8.96	57.24 ± 11.21	56.69 ± 10.95	Group 3 > 1	<0.001*	Group 2 > 3	0.691
8	71.60 ± 16.62	65.91 ± 15.13	74.06 ± 17.18	70.96 ± 15.70	Group 3 > 1	0.039*	Group 2 > 3	0.132
7	126.19 ± 27.24	123.33 ± 30.00	131.83 ± 25.08	118.15 ± 26.97	Group 1 > 3	0.243	Group 2 > 3	< 0.001†
6 Inferior	114.38 ± 24.13	123.33 ± 30.01	117.84 ± 23.62	106.14 ± 22.11	Group 1 > 3	0.002*	Group 2 > 3	< 0.001†
5	85.86 ± 17.87	86.67 ± 18.68	88.04 ± 18.37	81.51 ± 15.71	Group 1 > 3	0.063	Group 2 > 3	0.003†
4	59.15 ± 11.32	60.52 ± 9.42	60.25 ± 12.75	56.35 ± 9.19	Group 1 > 3	0.005*	Group 2 > 3	0.003†
3 Nasal	55.60 ± 10.10	56.27 ± 10.14	56.04 ± 11.02	54.39 ± 8.22	Group 1 > 3	0.184	Group 2 > 3	0.149
2	73.70 ± 13.34	75.90 ± 13.10	74.99 ± 14.22	70.03 ± 11.07	Group 1 > 3	0.003*	Group 2 > 3	0.002†
1	99.52 ± 22.00	103.16 ± 25.90	101.37 ± 21.58	93.92 ± 18.96	Group 1 > 3	0.013*	Group 2 > 3	0.003†
ONH parameters								
Rim area (mm^2)	1.04 ± 0.22	0.94 ± 0.19	1.11 ± 0.23	0.98 ± 0.20	Group 3 > 1	0.142	Group 2 > 3	< 0.001†
Disc area (mm^2)	2.01 ± 0.41	2.12 ± 0.36	2.01 ± 0.42	1.94 ± 0.41	Group 1 > 3	0.003*	Group 2 > 3	0.198
Average C/D ratio	0.67 ± 0.11	0.72 ± 0.08	0.64 ± 0.11	0.68 ± 0.10	Group 1 > 3	0.002*	Group 3 > 2	0.008†
Vertical C/D ratio	0.64 ± 0.11	0.69 ± 0.09	0.61 ± 0.11	0.65 ± 0.11	Group 1 > 3	0.008*	Group 3 > 2	0.012†
Cup volume (mm^3)	0.37 ± 0.25	0.53 ± 0.32	0.33 ± 0.22	0.35 ± 0.22	Group 1 > 3	<0.001*	Group 3 > 2	0.483

* Value for comparison of nonmyopic and myopic preperimetric glaucomatous eyes using Student's *t*-test.
† Value for comparison of myopic healthy eyes and myopic preperimetric glaucomatous eyes using Student's *t*-test.
‡ The clock-hour sectors were assessed in a clockwise direction for right eyes and in a counterclockwise direction for left eyes, with the temporal sector set at 9 o'clock.

Table 3. Discriminating Ability of Macular GCIPL Thickness Parameters, Peripapillary RNFL Thickness Parameters, and ONH Parameters

Parameters	AUROC (95% CI)
Macular GCIPL thickness parameters, μm	
Average	0.703 (0.639–0.766)
Minimum	0.702 (0.638–0.767)
Superotemporal	0.652 (0.583–0.720)
Superior	0.647 (0.581–0.713)
Superonasal	0.623 (0.557–0.690)
Inferonasal	0.638 (0.571–0.706)
Inferior	0.702 (0.639–0.765)
Inferotemporal	0.752 (0.692–0.811)
Main RNFL thickness parameters, μm	
Average	0.677 (0.614–0.740)
Superior	0.601 (0.534–0.668)
Nasal	0.624 (0.559–0.688)
Inferior	0.686 (0.623–0.749)
Temporal	0.561 (0.492–0.629)
RNFL clock-hour thickness parameters, μm	
12 Superior	0.564 (0.496–0.632)
11	0.543 (0.473–0.614)
10	0.593 (0.526–0.660)
9 Temporal	0.500 (0.431–0.569)
8	0.538 (0.469–0.607)
7	0.648 (0.581–0.715)
6 Inferior	0.656 (0.590–0.721)
5	0.615 (0.548–0.683)
4	0.599 (0.532–0.665)
3 Nasal	0.539 (0.472–0.606)
2	0.603 (0.537–0.669)
1	0.598 (0.531–0.664)
ONH parameters	
Rim area (mm^2)	0.655 (0.589–0.720)
Disc area (mm^2)	0.550 (0.481–0.619)
Average C/D ratio	0.403 (0.335–0.468)
Vertical C/D ratio	0.400 (0.331–0.468)
Cup volume (mm^3)	0.471 (0.402–0.539)

CI, confidence interval.

* The clock-hour sectors were assessed in a clockwise direction for right eyes and in a counterclockwise direction for left eyes, with the temporal sector set at 9 o'clock.

area AUROCs were 0.655, 0.643, and 0.672 in the total, nonhighly, and highly myopic groups, respectively. Between the nonhighly and highly myopic groups, there were no significant AUROC value differences.

Considering the performances of all of the peripapillary RNFL thickness, macular GCIPL thickness, and ONH parameters, inferotemporal GCIPL thickness demonstrated the best diagnostic ability. In the total myopic group, there were statistically significant differences between the best GCIPL thickness parameter (the inferotemporal GCIPL parameter) and the others (Table 4, Supplementary Table S3).

Figures 1 and 2 show cases of PPG with a localized RNFL defect in a nonhighly myopic and a highly myopic eye, respectively. A pseudo RNFL defect caused by a temporal shifting of the peak of the RNFL thickness curve should be considered when interpreting the OCT result in the highly myopic eyes (Fig. 2). In that sense, the macular GCIPL thickness, especially inferotemporal thickness, showed more reliable and better ability to detect PPG in myopic eyes than RNFL analysis.

Table 4. Comparison of AUROC Curves Between Inferotemporal GCIPL Thickness and Other Parameters

Parameters	AUROC (95% CI)	*P* Value
Average RNFL	0.677 (0.697–0.801)	0.021*
Inferotemporal GCIPL	0.752 (0.697–0.801)	
Average GCIPL	0.703 (0.646–0.755)	0.012*
Inferotemporal GCIPL	0.752 (0.697–0.801)	
Rim area	0.655 (0.596–0.710)	0.016*
Inferotemporal GCIPL	0.752 (0.697–0.801)	
Inferior RNFL	0.686 (0.629–0.739)	0.036*
Inferotemporal GCIPL	0.752 (0.697–0.801)	
Minimum GCIPL	0.702 (0.646–0.755)	0.013*
Inferotemporal GCIPL	0.752 (0.697–0.801)	

* Comparison was performed using the method of DeLong et al.[23]

Discussion

Diagnosis of glaucoma in cases of myopia is important, though in clinical practice, the structural changes related to myopia, such as disc tilt, shallow cupping, and large peripapillary crescent, render precise diagnosis difficult.[4,17] Clinical diagnosis of glaucoma is especially difficult in patients without definite VF loss, given the often unusual appearance of the optic disc.

Many studies have demonstrated that SD-OCT measurement of macular ganglion cell complex (GCC) thickness offers a glaucoma detection ability comparable in effectiveness to that for peripapillary RNFL thickness.[11–16,24,25] Ganglion cell complex is defined as the sum of the three innermost retinal layers, namely the RNFL, ganglion cell layer (GCL), and inner plexiform layer (IPL). In the present study, we used a GCA algorithm to measure, by SD-OCT, the thickness of the macular GCIPL. The thickness of the GCIPL is the sum of the GCL and IPL, and, thus, importantly, is less influenced by RNFL thickness variation than is GCC thickness.[18] Furthermore, previous studies have shown not only that the GCA algorithm of the Cirrus SD-OCT can measure macular GCIPL thickness successfully, but also that its glaucoma detection ability is comparable to that of the peripapillary RNFL thickness and ONH parameters.[26–28] In our study, the mean AUROC range was 0.623 to 0.752 for the GCIPL parameters, approximately 0.500 to 0.686 for the RNFL parameters, and approximately 0.400 to 0.655 for the ONH parameters,. Thus, the GCIPL parameters showed better diagnostic ability than either the RNFL or ONH parameters. Among all of the SD-OCT parameters, moreover, inferotemporal GCIPL thickness was the best for detection of PPG. The best individual parameters were inferotemporal GCIPL among the GCIPL parameters, inferior RNFL among the RNFL parameters, and rim area among the ONH parameters. Inferotemporal GCIPL thickness showed significant differences relative to all of the other best parameters, such as inferior RNFL thickness and rim area ($P = 0.036$, 0.016, respectively). The AUROCs of inferotemporal GCIPL thickness were 0.752 in the total, 0.747 in the nonhighly, and 0.737 in the highly myopic groups.

Evaluation of GCIPL parameters in PPG eyes has been rare.[28–30] Begum et al.[28] reported that, for perimetric glaucoma, the diagnostic ability of the GCIPL parameters was similar to that of the RNFL and ONH parameters; however, for PPG, the GCIPL parameters' diagnostic effectiveness was significantly lower than those of the RNFL and ONH parameters. Other studies conducted in Korea have shown somewhat different results, in that the GCIPL parameters were as good as the RNFL and ONH parameters in diagnosing PPG.[29,30] As for other Korean studies, Na et al.[5] reported a

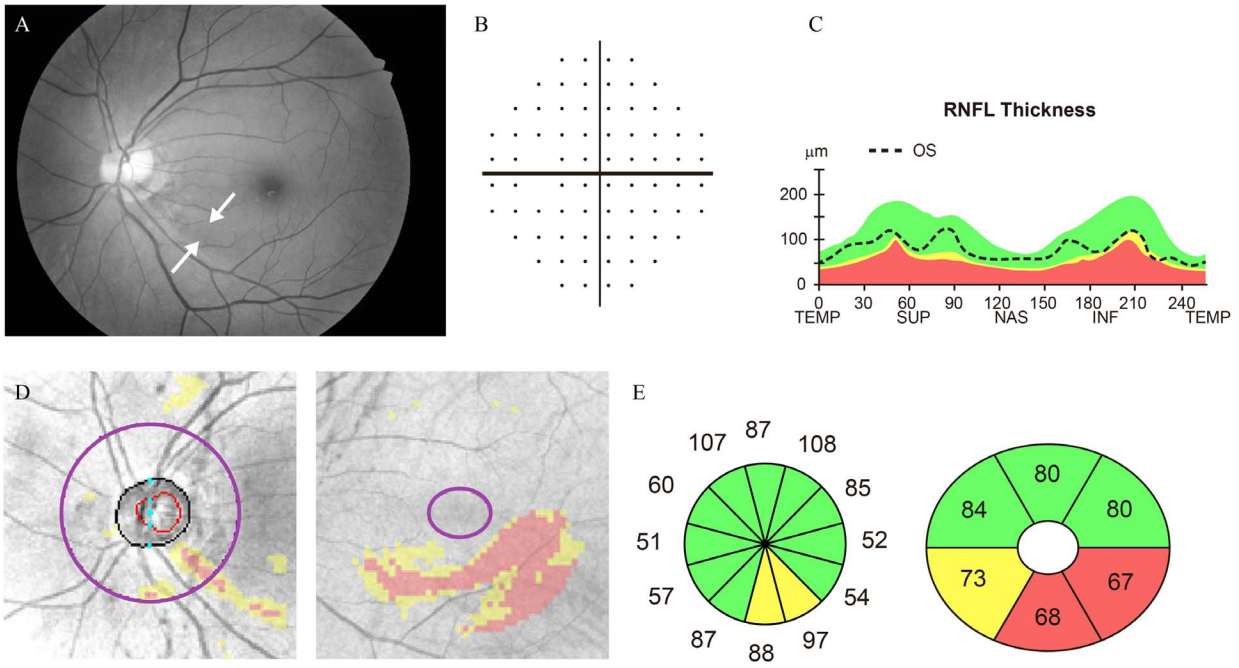

Figure 1. A 46-year-old female in the nonhighly myopic group had preperimetric glaucoma with a localized RNFL defect. The spherical equivalent was −5.63 D and the AXL was 26.82 mm. (**A**) Red-free fundus photography showed an inferotemporal localized RNFL defect (between the *arrows*). (**B**) Visual field by standard automated perimetry was normal. (**C**) Retinal nerve fiber layer thickness curve showed thinning of the inferotemporal RNFL. (**D**) Peripapillary RNFL deviation map and GCIPL deviation map showed a significant thinning in the corresponding inferior region. (**E**) The defects were detected by RNFL clock-hour and GCIPL sector analyses.

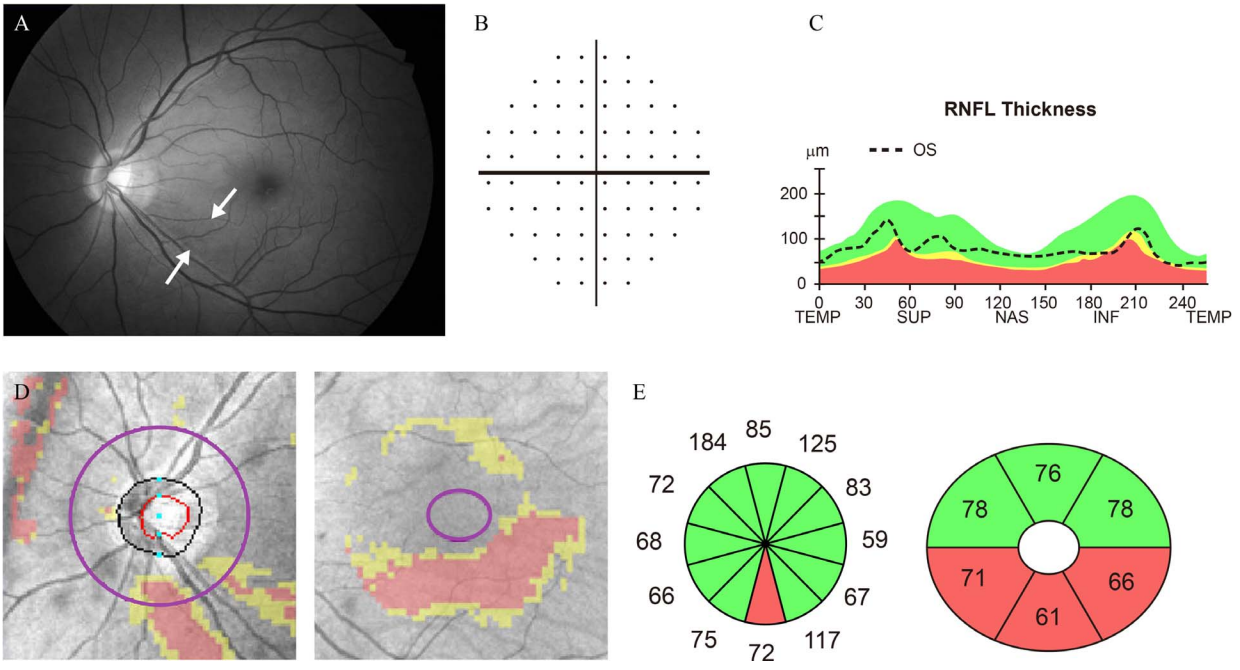

Figure 2. A 44-year-old male in the highly myopic group had preperimetric glaucoma with localized RNFL defect. The spherical equivalent was −7.00 D and the AXL was 28.21 mm. (**A**) Red-free fundus photography showed an inferotemporal localized RNFL defect (between the *arrows*). (**B**) Visual field by standard automated perimetry was normal. (**C**) The RNFL thickness curve showed thinning of inferotemporal RNFL. (**D**) Peripapillary RNFL deviation map and GCIPL deviation map showed a significant thinning in the corresponding inferior region. (**E**) The defects were detected by RNFL clock-hour and GCIPL sector analyses. The inferior defect in the RNFL deviation map ([**D**], *left*) and the 6 o'clock defect in the RNFL clock-hour analysis ([**E**], *left*) seemed to be caused by the temporal shifting of the inferior peak RNFL thickness curve (**C**) which is typically seen in highly myopic eyes.

Investigative Ophthalmology & Visual Science

significant GCIPL thickness difference between PPG and healthy control eyes, which fact might suggest that macular GCIPL thickness can serve as an early indicator of glaucomatous structural damage. Begum et al.[28] explained that a possible reason for the greater diagnostic abilities of GCIPL parameters in respect to the Korean population might be due to the location of glaucomatous damage being closer to the fovea. They cited previous studies that showed a higher prevalence of normal-tension glaucoma (NTG) in the Korean population along with glaucomatous damage closer to fixation.[31,32] Kim et al.[30] reported similar results; that is, the diagnostic ability of GCIPL parameters increased where the RNFL defects were closer to the fovea.

In our results, the diagnostic abilities of the macular GCIPL parameters were comparable to those of the other parameters. This finding is consistent with the other, previous reports from Korea. We found that inferotemporal GCIPL thickness showed the highest value of AUROC as well as statistically significant differences with the other parameters, such as inferior RNFL (the best RNFL parameter) or rim area (the best ONH parameter). This result, however, is somewhat different from those of some of the previous reports. Kim et al.[10] for example, reported that inferotemporal, minimum, and average GCIPL thickness showed the best diagnostic performances; yet there were no significant difference among the AUROCs of the GCIPL, RNFL, and ONH parameters. Given that our study included only myopic eyes, it might be true that, especially in myopic eyes, the inferotemporal GCIPL parameter is the most useful for differentiation of glaucomatous from healthy eyes. In the highly myopic group, inferotemporal GCIPL thickness, compared to the other parameters, did not show any significantly better ability to detect PPG. One of the reasons for this might be the small number of subjects in the highly myopic group or the relatively low AUROC value for inferotemporal GCIPL thickness. Still, despite the lack of any significant difference between inferotemporal GCIPL thickness and other parameters, we assume the GCIPL parameter to be important for diagnosis of glaucoma in highly myopic eyes, because the average, inferior, and inferotemporal GCIPL parameters only showed AUROC values over 0.7 in the highly myopic group.

Some reports on glaucoma diagnosis for myopic eyes have shown conflicting results.[6–10] Kim et al.[11] found the glaucoma detection ability of macular GCC thickness to be comparable to that of peripapillary RNFL for highly myopic subjects. Shoji et al.[15] determined that for glaucoma detection in highly myopic eyes, global volume loss of macular GCC provided a significantly better AUROC than did average peripapillary RNFL thickness. Another study, by Shoji et al.,[16] showed that macular GCC measurement efficiently detected glaucoma in the highly myopic and emmetropia groups, whereas the ability of peripapillary RNFL measurement in the highly myopic group was inferior to that in the emmetropia group. In considering our current results, we concluded that for myopic eyes, careful evaluation of inferotemporal GCIPL thickness can be helpful for differentiating PPG eyes from healthy eyes. Recently, Na et al.[33] reported that perimetric glaucoma and PPG eyes, as assessed by Cirrus SD-OCT, showed different macular thickness progression rates and patterns. They also noted that among the macular thickness parameters, the inferior outer sector showed the highest progression rate. This is in accordance with the earlier study results as well as our present ones, which indicated that the inferior quadrant and inferior outer sector are the most diagnostically sensitive sectors.[30,34]

We compared all of the parameters between the NGE and MGE and MHE and MGE. As shown in Table 2, in the comparison between the MHE and MGE, the MGE showed thinner thickness in all of the macular GCIPL thickness and RNFL thickness parameters. However, the differences separating those with from those without glaucoma were small. The differences in some parameters, for example, were only 3 to 4 μm. Given these results, we can expect that such small differences do, indeed, determine disease or health. In the comparison between the NGE and MGE, the MGE was thinner than the NGE in all of the parameters other than the temporal region of the RNFL. These results are in accordance with the relevant previous reports.[5–10,36,37] Many of those studies reported that the RNFL was thinner in myopic eyes than in nonmyopic eyes.[5–10] With respect to temporal RNFL thickness in myopia, some studies found that RNFL thickness was least affected by AXL in that region and was even increased.[6,36,37] Kang et al. [9] similarly reported that myopia might be associated with temporal deviations of peak RNFL thickness, which phenomenon might have caused the temporal RNFL thickening noted in the current study.

The current study has two limitations. First, its design is retrospective. Second, the number of subjects in the highly myopic group was relatively small (27 glaucomatous and 33 healthy eyes) relative to the nonhighly myopic group (77 glaucomatous and 149 healthy eyes). For fruitful further investigation, a prospective study with larger numbers of highly myopic eyes will be required.

In summary, the inferotemporal macular GCIPL thickness parameter was the best for detection of PPG in myopic eyes. Certainly, our results suggested that clinicians must focus on this measure in differentiating PPG from healthy eyes in myopic patients.

Acknowledgments

Disclosure: **B.R. Seol**, None; **J.W. Jeoung**, None; **K.H. Park**, None

References

1. Grossniklaus HE, Green WR. Pathologic findings in pathologic myopia. *Retina*. 1992;12:127–133.
2. Chihara E, Chihara K. Covariation of optic disc measurements and ocular parameters in the healthy eye. *Graefes Arch for Clin Exp Ophthalmol*. 1994;232:265–271.
3. Jonas JB, Dichtl A. Optic disc morphology in myopic primary open-angle glaucoma. *Graefes Arch for Clin Exp Ophthalmol*. 1997;235:627–733.
4. Tay E, Seah SK, Chan SP, et al. Optic disk ovality as an index of tilt and its relationship to myopia and perimetry. *Am J Ophthalmol*. 2005;139:247–252.
5. Na JH, Sung KR, Baek S, et al. Detection of glaucoma progression by assessment of segmented macular thickness data obtained using spectral domain optical coherence tomography. *Invest Ophthalmol Vis Sci*. 2012;53:3817–3826.
6. Leung CKS, Mohamed S, Leung KS, et al. Retinal nerve fiber layer measurements in myopia: an optical coherence tomography study. *Invest Ophthalmol Vis Sci*. 2006;47:5171–5176.
7. Rauscher FM, Sekhon N, Feuer WJ, Budenz DL. Myopia affects retinal nerve fiber layer measurements as determined by optical coherence tomography. *J Glaucoma*. 2009;18:501–505.
8. Hong SW, Ahn MD, Kang SH, Im SK. Analysis of peripapillary retinal nerve fiber distribution in normal young adults. *Invest Ophthalmol Vis Sci*. 2010;51:3515–3523.
9. Kang SH, Hong SW, Im SK, Lee SH, Ahn MD. Effect of myopia on the thickness of the retinal nerve fiber layer measured by Cirrus HD optical coherence tomography. *Invest Ophthalmol Vis Sci*. 2010;51:4075–4083.
10. Kim MJ, Lee EJ, Kim TW. Peripapillary retinal nerve fiber layer thickness profile in subjects with myopia measured using the

Stratus optical coherence tomography. *Br J Ophthalmol*. 2010;94:115–120.

11. Kim NR, Lee ES, Seong GJ, et al. Comparing the ganglion cell complex and retinal nerve fiber layer measurements by Fourier domain OCT to detect glaucoma in high myopia. *Br J Ophthalmol*. 2011;95:1115–1121.
12. Rao H, Babu J, Addepalli U, et al. Retinal nerve fiber layer and macular inner retina measurements by spectral domain optical coherence tomography in Indian eyes with early glaucoma. *Eye*. 2012;26:133–139.
13. Seong M, Sung KR, Choi EH, et al. Macular and peripapillary retinal nerve fiber layer measurements by spectral domain optical coherence tomography in normal-tension glaucoma. *Invest Ophthalmol Vis Sci*. 2010;51:1446–1452.
14. Tan O, Chopra V, Lu ATH, et al. Detection of macular ganglion cell loss in glaucoma by Fourier-domain optical coherence tomography. *Ophthalmology*. 2009;116:2305–2314.
15. Shoji T, Sato H, Ishida M, Takeuchi M, Chihara E. Assessment of glaucomatous changes in subjects with high myopia using spectral domain optical coherence tomography. *Invest Ophthalmol Vis Sci*. 2011;52:1098–1102.
16. Shoji T, Nagaoka Y, Sato H, Chihara E. Impact of high myopia on the performance of SD-OCT parameters to detect glaucoma. *Graefes Arch for Clin Exp Ophthalmol*. 2012;250:1843–1849.
17. Özdek SC, Önol M, Gürelik G, Hasanreisoglu B. Scanning laser polarimetry in normal subjects and patients with myopia. *Br J Ophthalmol*. 2000;84:264–267.
18. Choi YJ, Jeoung JW, Park KH, Kim DM. Glaucoma detection ability of ganglion cell-inner plexiform layer thickness by spectral-domain optical coherence tomography in high myopia. *Invest Ophthalmol Vis Sci*. 2013;54:2296–2304.
19. Mwanza JC, Oakley JD, Budenz DL, Chang RT, Knight OJ, Feuer WJ. Macular ganglion cell–inner plexiform layer: automated detection and thickness reproducibility with spectral domain–optical coherence tomography in glaucoma. *Invest Ophthalmol Vis Sci*. 2011;52:8323–8329.
20. Mwanza JC, Durbin MK, Budenz DL, et al. Profile and predictors of normal ganglion cell–inner plexiform layer thickness measured with frequency-domain optical coherence tomography. *Invest Ophthalmol Vis Sci*. 2011;52:7872–7879.
21. Curcio CA, Allen KA. Topography of ganglion cells in human retina. *J Comp Neurol*. 1990;300:5–25.
22. Savini G, Carbonelli M, Barboni P. Spectral-domain optical coherence tomography for the diagnosis and follow-up of glaucoma. *Curr Opin Ophthalmol*. 2011;22:115–123.
23. DeLong ER, DeLong DM, Clarke-Pearson DL. Comparing the areas under two or more correlated receiver operating characteristic curves: a nonparametric approach. *Biometrics*. 1988;44:837–845.
24. Garas A, Vargha P, Hollo G. Diagnostic accuracy of nerve fiber layer, macular thickness and optic disc measurements made with the RTVue-100 optical coherence tomography to detect glaucoma. *Eye*. 2011;25:57–65.
25. Schulze A, Lamparter J, Pfeiffer N, Berisha F, Schmidtmann I, Hoffmann EM. Diagnostic ability of retinal ganglion cell complex, retinal nerve fiber layer, and optic nerve head measurements by Fourier-domain optical coherence tomography. *Graefes Arch Clin Exp Ophthalmol*. 2011;249:1039–1045.
26. Mwanza JC, Durbin MK, Budenz DL, et al. Glaucoma diagnostic accuracy of ganglion cell–inner plexiform layer thickness: comparison with nerve fiber layer and optic nerve head. *Ophthalmology*. 2012;119:1151–1158.
27. Takayama K, Hangai M, Durbin M, et al. A novel method to detect local ganglion cell loss in early glaucoma using spectral-domain optical coherence tomography. *Invest Ophthalmol Vis Sci*. 2012;53:6904–6913.
28. Begum VU, Addepalli UK, Yadav RK, et al. Ganglion cell-inner plexiform layer thickness of high definition optical coherence tomography in perimetric and preperimetric glaucoma. *Invest Ophthalmol Vis Sci*. 2014;55:4768–4775.
29. Sung MS, Yoon JH, Park SW. Diagnostic validity of macular ganglion cell-inner plexiform layer thickness deviation map algorithm using cirrus HD-OCT in preperimetric and early glaucoma. *J Glaucoma*. 2014;23:144–151.
30. Kim MJ, Jeoung JW, Park KH, Choi YJ, Kim DM. Topographic profiles of retinal nerve fiber layer defects affect the diagnostic performance of macular scans in preperimetric glaucoma. *Invest Ophthalmol Vis Sci*. 2014;55:2079–2087.
31. Kim CS, Seong GJ, Lee NH, Song KC. Prevalence of primary open-angle glaucoma in central South Korea: the Namil study. *Ophthalmology*. 2011;118:1024–1030.
32. Kim DM, Seo JH, Kim SH, Hwang SS. Comparison of localized retinal nerve fiber layer defects between a low-teen intraocular pressure group and a high-teen intraocular pressure group in normal-tension glaucoma patients. *J Glaucoma*. 2007;16:293–296.
33. Na JH, Sung KR, Baek SH, Kim ST, Shon K, Jung JJ. Rates and patterns of macular and circumpapillary retinal nerve fiber layer thinning in preperimetric and perimetric glaucomatous eyes. *J Glaucoma*. 2015;24:278–285.
34. Sung KR, Kim DY, Park SB, Kook MS. Comparison of retinal nerve fiber layer thickness measured by Cirrus HD and Stratus optical coherence tomography. *Ophthalmology*. 2009;116:1264–1270.
35. Vernon SA, Rotchford AP, Negi A, Ryatt S, Tattersal C. Peripapillary retinal nerve fiber layer thickness in highly myopic Caucasians as measured by Stratus optical coherence tomography. *Br J Ophthalmol*. 2008;92:1076–1080.
36. Hougaard JL, Ostenfeld C, Heijl A, Bengtsson B. Modelling the normal retinal nerve fiber layer thickness as measured by stratus optical coherence tomography. *Graefes Arch Clin Exp Ophthalmol*. 2006;224:1607–1614.
37. Choi S, Lee S. Thickness changes in the fovea and peripapillary retinal nerve fiber layer depend on the degree of myopia. *Korean J Ophthalmol*. 2006;20:215–219.

Investigative Ophthalmology & Visual Science